www.vbripress.com/aml, DOI: 10.5185/amlett.2016.6061

Low cost biosorbents based on modified starch iron oxide nanocomposites for selective removal of some heavy metals from aqueous solutions

Abdul-Raheim M. Abdul-Raheim, El-Saeed Shimaa M., Farag Reem K., Abdel-Raouf Manar E.*

Petroleum Application Department, Egyptian Petroleum Research Institute, 1 Ahmed El-Zomor street,
Nasr city, Cairo, 11727, Egypt

*Corresponding author. Tel: (+20) 2227-45902; E-mail: drmanar770@yahoo.com

Received: 15 July 2015, Revised: 09 December 2015 and Accepted: 15 March 2016

ABSTRACT

In this work, the starch extracted from potato peels was modified with acrylic acid. Nanoparticles composed of modified starch polymer and Fe_3O_4 (modified potato starch-magnetic nanoparticles, MPS-MNPs) were synthesized. The prepared nanoadsorbents were used for selective exclusion of Pb^{2+}, Cu^{2+}, and Ni^{2+} ions from water. They were characterized by different analytical instruments such as FTIR, TEM and XRD. Adsorption of all captured metal ions onto MPS-MNPs was observed to be reliant on temperature, pH and contact time. Clump adsorption balance was come to in 60 min and most extreme uptakes for Cu^{2+}, Pb^{2+} and Ni^{2+} in non-aggressive adsorption mode were 100, 70 and 100 mgg^{-1}, respectively at 35 °C. In focused adsorption tests, PS-MNPs specially adsorbed Ni^{2+}ions with an affinity order of $Ni^{2+}>Cu^{2+}>Pb^{2+}$. The effect of monomer and initiator concentrations on grafting process was studied. Furthermore, the recyclability of PS-MNPs was investigated.

Keywords: Heavy metals; potato starch; low cost; adsorbents; magnetic nanoparticles.

Introduction

Water pollution because of toxic heavy metals is a matter of great concern due to their unfavorable impacts on both the earth and human wellbeing. Heavy metals particles, for example, lead (Pb^{2+}), nickel (Ni^{2+}) and copper (Cu^{2+}) are poisonous and cancer-causing at even low fixations, **Table 1**. Substantial metals are non-biodegradable and they can collect in living life forms.

Table 1. The hazardous effects of some heavy metals.

Heavy metal	Toxicities	MCL(mg/L)
Mercury	Diseases of kidneys, circulatory system, nervous system and Rheumatoid arthritis	0.00003
Lead	Harm circulatory, nervous system, harm the fetal brain, diseases of the kidneys.	0.006
Zinc	Lethargy, neurological signs increased thirst and Depression.	0.80
Nickel	Nausea, Dermatitis,, coughing, chronic asthma and human carcinogen	0.20
Copper	Liver failure, Wilson disease and insomnia	0.25
Chromium	Headache, diarrhea, nausea, vomiting, carcinogenic	0.05
Cadmium	Kidney failure, renal disorder, human carcinogen	0.01
Arsenic	Skin manifestations, visceral cancers, vascular disease	0.050

They are by and large released to nature from different mechanical exercises, for example, purifying, electroplating, painting, mining, calfskin tanning, composite and battery producing, and so on., representing a noteworthy risk to the earth and general wellbeing [**1**]. Therefore, reliable methods are necessary for the removal of heavy metals from aquatic environment.

An extensive exertion has been dedicated to the viable removal of heavy metal particles from environment. There are different treatment procedures accessible for removal of dangerous metals such as chemical precipitation, coagulation, ion exchange, adsorption, electrolysis reverse, osmosis, film process, and so on [**2-4**].

Among every one of these strategies, adsorption is viewed as a successful, productive and economic strategy for the removal of various contaminations from wastewater. Also, adsorption is all inclusive and quick in nature and pertinent for the removal of natural and inorganic toxins even at low concentration [**5-8**].

Development of new generation environmental friendly adsorbent based on natural nano materials is the current research interest [**9**].

In the process of elimination of heavy metals from waste water, natural polymers, principally polysaccharides, for example, starch and its subordinates, chitosan, cyclodextrin have pulled specifically considerations, because of their physical and chemical properties, minimal effort, accessibility and the existence of different reactive groups on their chemical structure [**10, 11**]. In spite of their importance, they have a few hindrances that point of confinement their utilization, for example, their low surface area and difficulty of separation from solution. Conversely, magnetic sorbents have a moderately high surface area and are anything but difficult to isolated and control in complex multiphase systems with an outer magnetic field [**12**].

Hybrid (organic and inorganic) composites of high stability can be obtained by incorporating a natural polymer in an inorganic nano material along these lines joining the upsides of both materials. Composites made from various polysaccharides constitute another category of naturally safe materials for diverse biological and industrial applications. It was mentioned that magnetic nano-materials functionalized with biopolymers, for example, chitosan [**13**], gum Arabic [**14**], cellulose [**15**] and chitosan [**16, 17**] have been utilized for the exclusion of toxic metals from aqueous solution.

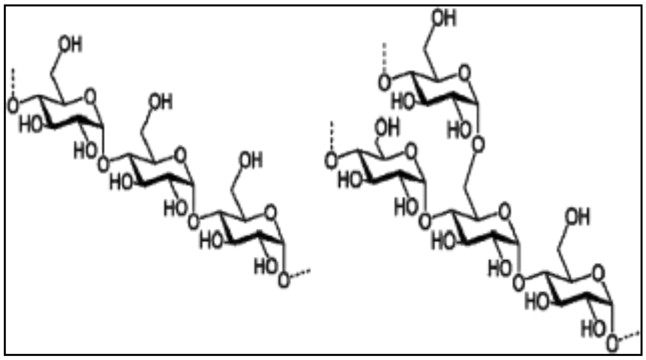

Fig. 1. Molecular structures of starch (left: amylose; right: amylopectin).

Starch is a polysaccharide which consists of repeating D-glucopyranose units, linked together by α-1, 4 linkages, **Fig. 1**. Starch materials themselves are not really suitable as sorbents, since they need controllable molecule size and certain wear resistance, hardness, and porosity; however, it has been utilized for the elimination of substantial metal particles in different changed structures [**18-22**]. This renewable and biodegradable compound can complex different metal particles this complexation capacity can be enhanced by modifying starch with suitable useful groups via esterification, cross-linking and oxidation reaction of hydroxyls in the interior cavities [**23-28**].

In order to crosslink polymers containing hydroxyl groups on their backbones , such as starch, the cross linkers must have a tendency to react with two hydroxyl groups at least in a single polymer molecule or in another adjacent molecules. For starch crosslinking, bifunctional and multifunctional reagents are normally used to form ether, ester or other linkages with the hydroxyl groups in starch molecules [**29**]. By varying crosslinker dosages, starch concentration, pH and temperatures, the extent of crosslinking could be controlled. In addition, the crosslinking of starch can also be achieved by irradiation without any additives, which is normally used in grafting processes [**30**].

Compared to native starches, crosslinked starches have superior properties in aspects of mechanical, thermal and chemical resistance, such as an improved viscosity, better textural properties, and a higher resistance to high temperature, low pH, and high shear force [**31**]. Therefore, crosslinked starch hydrogels have many applications, in food, oilfield, pharmaceutical, water treatment and other industries [**32**].

The aim of this work is to prepare modified starch nanocomposite by reaction with acrylic acid and application of the modified starch as absorbent for heavy metals from aqueous media under different conditions. Furthermore, the influences of process parameters such as monomer and initiator concentrations on the graft polymerization of acrylic acid to potato starch were investigated.

Materials and methodology

Iron(II)chloride tetrahydrate (99 %), iron (III) chloride hexahydrate (98 %), Benzoyl peroxide (BPO) and Acrylic acid were purchased from Sigma-Aldrich. Lead(II) nitrate, ammonium hydroxide (25 %), nickel(II)nitrate and Copper(II) nitrate were purchased from Merck [MA, USA]. All the chemicals are analytical grade chemicals and used as received without additional purification. Potato starch was obtained from potato peels after treatment. Potato peels were chosen as biomaterial because of their chemical stability, non-catalytic activity and local availability at very low cost.

Sample preparation and pre-treatment

Potato peels were washed repeatedly with distilled water followed by filtration so as to eliminate dust and soluble impurities. The washed samples were oven dried at 100 ^{o}C to constant weight. The cleaned samples were then ground into powder and sieved to 150 – 250 µm particle size. The chemically activated samples were prepared by boiling starch powder in 0.1M NaOH for an hour at room temperature (70 ^{o}C). The waste slurry was then heated to 120 ^{o}C. Then it was washed many times by distilled water to remove any extra base until the water comes out becomes neutral after that dried at 100 ^{o}C to constant weight.

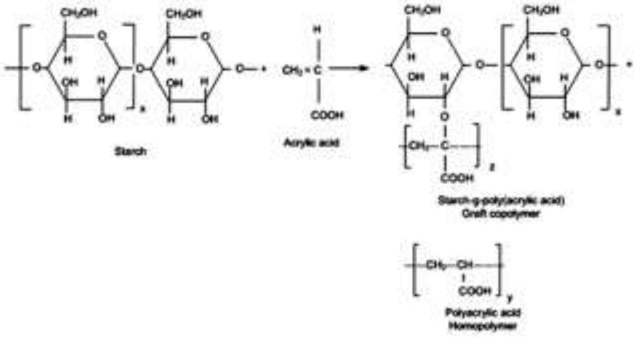

Scheme 1. Grafting of acrylic acid into starch.

Graft copolymerization of acrylic acid onto treated potato starch (synthesis of starch-g-poly(AAc))

Synthesis of graft copolymer is exposed in **Scheme 1**. in 100 ml distilled water with 0.1 N NaOH (0.4 g) solution 1.0 gram of the treated potato starch (TPS) was dissolved, then, stirred for 60 minutes at 70 ºC, before grafting was carried out using monomer. Unmistakable measure of initiator (benzoyl peroxide) was added to the response blend and permitted to react with starch for 10 minutes. From that point, clear measure of acrylic acid was included into the reaction blend with consistently mixing at a specific temperature (70 $^{\circ}$C) for six hours. Subsequent to cooling, the 25 ml ethanol was poured into the above reaction mixture to precipitate it. Then, the reaction blend was kept at room temperature for 24 hours. The precipitates obtained were filtered off and dried in a hot air oven at 60 ºC and weighed precisely. Several reaction parameters for example concentration and initiator concentration were optimized to get maximum graft yield. Synthesized graft copolymers were washed comprehensively with acetone and then with distilled water to eliminate attached homopolymer from graft copolymer. Finally, they were dried in a hot air oven at 50 ºC. Synthesized graft copolymers were studied in metal ion removal.

Table 2. Different reaction parameters.

Monomer type	Monomer concentration	Initiator type	Initiator concentration
Acrylic acid Acrylonitril Acrylic acid/ Acrylonitril (1:1,1:3and 3:1)	0.5, 1, 1.5, 2 and 2.5 wt: wt % of the starch	Chromic acid (CA) Benzoylperoxide (BPO)	0.01- 0.05 % of the monomer concentration

Different reaction parameters are summarized in **Table 2**. Percentage of grafting yield and also grafting efficiency of starch-g-poly(Acrylic acid) were calculated by using the following equations:

$$\text{Grafting yield (\%)} = (W3-W1)/W1 \text{ X } 100 \qquad (1)$$

$$\text{Grafting efficiency (\%)} = (W3-W1)/W2 \text{ X}100 \qquad (2)$$

where, W1 is the weight of starch before grafting, W2 is the weight of Acrylic acid before grafting and W3 is the total weight after grafting Acrylic acid onto the starch.

Synthesis of starch-g-poly(AAc), coated magnetic nanoparticles (MPS-MNPs)

MPS-MNPs were synthesized by single step co-precipitation technique. Shortly, 2.36 g $FeCl_3{\cdot}6H_2O$, 0.86 g of $FeCl_2{\cdot}4H_2O$, and 1.5 g starch-g-poly (AAc) were dissolved in 40 mL of distilled water with vigorous stirring at 1000 rpm. After the solution was heated to 90 °C, 5 mL of 25 % NH_4OH was added. The reaction was continued for 1 h at 90 °C under constant stirring and nitrogen environment. The resulting nanoparticles were then washed with distilled water six times to remove the unreacted chemicals and dried in a vacuum oven. The codes and the compositions of the prepared nanocomposites are given in **Table 3**.

Table 3. Codes and compositions of the prepared magnetic nanogels.

Code	Composition
MPS-MNP1	0.5 AA+ 0.01BPO +TPS+ Fe_2O_3
MPS-MNP2	0.5 AA+ 0.03BPO + TPS + Fe_2O_3
MPS-MNP3	0.5 AA+ 0.05BPO + TPS + Fe_2O_3
MPS-MNP4	1 AA+ 0.01BPO + TPS + Fe_2O_3
MPS-MNP5	1 AA+ 0.03BPO + TPS + Fe_2O_3
MPS-MNP6	1 AA+ 0.05BPO + TPS + Fe_2O_3
MPS-MNP7	1.5 AA+ 0.01BPO + TPS + Fe_2O_3
MPS-MNP8	1.5 AA+ 0.03BPO + TPS + Fe_2O_3
MPS-MNP9	1.5 AA+ 0.05BPO + TPS + Fe_2O_3

Characterization of the materials

- The functionalization of modified potato starch polymer onto the surface of Fe_3O_4 nanoparticle was recorded by (Perkin-Elmer720) with a KBr pellet infrared spectrometer (Model 400) over the range of 4000–400 cm^{-1}.
- Transmission electron microscope (TEM, Jeol2100, 200 Kv) was used to determine the size and morphology of magnetic particles.
- Thermo gravimetric analysis (TGA) was performed on a thermal analyzer (model Q600 SDT simultaneous DSC-TGA) to determine the magnetic content and thermal stability of the prepared MPS-MNPs. The X-ray diffraction (XRD) was carried out in a SHIMADZU diffractometer with high-intensity Cu Kα radiation (λ = 1.54065 Å) with the 2θ range from 10^o to 90^o.

Adsorption and desorption of heavy metal ions

Cu^{2+}, Ni^{2+} and Pb^{2+} ions adsorption test were conducted utilizing batch equilibrium method in aqueous medium at pH range 2 to 5.5 and at 25 to 55 °C. An average of 20 mg of dry magnetic nano adsorbents placed with 10 mL of Cu^{2+}, Pb^{2+}, and Ni^{2+}solution of 50 mg L^{-1} in a 50 ml bottles. The bottles were closed and shaken in a thermostatic shaker operated at 250 rpm for different time intervals 15, 30, 60, 90 and 120 minutes. Then the bottles were placed on permanent Nd–Fe–B magnet to remove magnetic nanoadsorbents and then the supernatant was obtained after magnetic decantation. The concentrations of Cu^{2+}, Ni^{2+} and Pb^{2+}ions were determined using flame atomic absorption spectrometer /ZEEnit 700P/Analytikjena Co. -Germany.

The solution pH was adjusted by 0.1N NaOH or 0.1N HCl. For the non-competitive tests, the initial Cu^{2+}, Ni^{2+} and Pb^{2+} ion concentrations used were 50 -250 mg L^{-1} and the pH utilized was 5.5. At different time intervals, samples were gathered after magnetic decantation and the concentration of contaminants were determined. In the competitive adsorption tests, the metal ions were added in equivalent amounts (each 50 mg L^{-1}) to a 10 mL solution enclosed in the vial. Then, vials were shaken for 2 h to guarantee equilibrium before the magnetic nanoparticles were removed and the concentrations of residual metal ions were measured as mentioned before. The removal efficiency of MPS-MNPs was calculated from the following relationship:

$$\%\ \text{Removal efficiency} = \frac{\text{The amount of cation Absorbed}}{\text{Initial cation Concentration}} \text{ X } 100 \qquad (3)$$

Desorption study was conducted using 0.01 M phosphoric acid as desorbing agent. It was inspected by adding 10 mL of the desorption eluent to the metal-sorbed MPS-MNPs. Subsequent to shaking at 250 rpm for 3 h, the solid phase MPS-MNPs were gathered by magnetic decantation and the concentration of each pollutant in the supernatant was measured. The reusability was checked by repeating the above adsorption–desorption process for four rounds.

Results and discussion

Synthesis and characterization of MPS-MNPS

Starch-g-poly(AAc), coated magnetic nanoparticles (MPS-MNPs) have been synthesized by simple co-precipitation of iron ions Fe^{2+} and Fe^{3+} and Starch-g-poly(AAc) polymer as shown in **Scheme 1**. Modification of Starch-g-poly(AAc) on magnetic nanoparticles was confirmed by FTIR spectroscopy. **Fig. 2**(**a**) shows the FTIR spectrum of starch extracted from potato peels, **Fig. 2**(**b**) shows the FTIR spectrum of Starch-g-poly(AAc) and **Fig. 2**(**c**) shows FTIR spectrum polymer coated Fe_3O_4 nanoparticles (MPS-MNP1) in the 4000–400 cm^{-1} wave number range. The most important characteristic peaks for each one and their interpretation are given in **Table 4**.

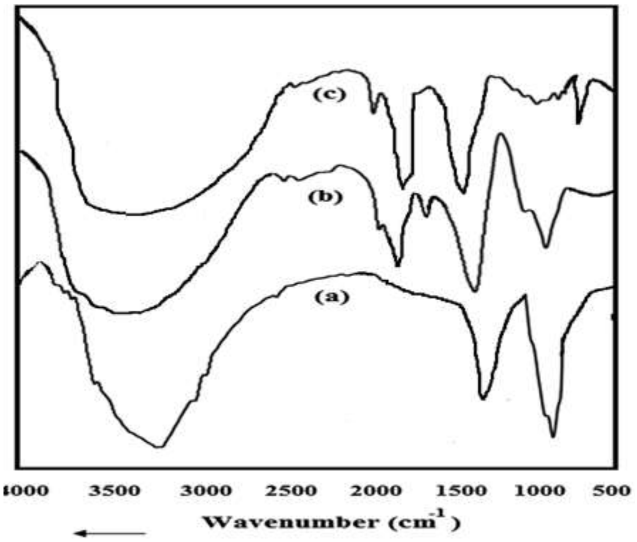

Fig. 2. FT-IR spectra of (a) Starch, (b) Starch-g-poly(AAc) and (c) MPS-MNP1.

Table 4. The most important peaks and their interpretation.

The compound	The most important peaks	Peak interpretation
Starch	A strong band at $2983cm^{-1}$	C-H stretching vibration assigned to the ether bonds
	A strong band at $1166cm^{-1}$	
	A strong absorption peak at $3323cm^{-1}$	O–H stretching of the hydroxyl groups of glucose unit
	A strong absorption band at 816 cm^{-1}	C–O stretching of alcohol
Starch-g-poly(AAc)	A strong band at 3200-3500 cm^{-1}	O–H stretching of carboxylic group
	A strong absorption band at 1780 cm^{-1}	C=O stretching vibration
MPS-MNP1	A wide strong band at 3200-3500 cm^{-1}	O–H stretching of carboxylic group
	A strong absorption band at 1780 cm^{-1}	C=O stretching vibration
	A strong peak at 590 cm^{-1}	Stretching vibration of Fe-O
	Two tops showed up at 1628 and 1400 cm^{1}	Bands of COOFe[**33**]

Grafting and fabrication of potato starch

The magnetite particle sizes and the effect of monomer and crosslinker concentration are illustrated in **Fig. 3**(**a-e**). **Fig. 3**(**a**) shows the TEM image for non-coated magnetite nanoparticles which show the largest particle size distribution with confirmation of aggregation of magnetite magnetic particles. **Fig. 3**(**b**) and (**c**) show the growth of polymer coating around magnetite in MPS-MNP1 and MPS-MNP2 as the percent of crosslinker increased from 0.01 to 0.03wt/wt of potato starch. **Fig. 3**(**d**) and (**e**) show complete polymer coating of MPS-MNP5 and MPS-MNP8 magnetite nanoparticles. TEM analysis showed that the production of magnetite with starch-g-poly(AAc) increases the size distribution of the magnetite nanoparticles and prevents particle aggregation because of the dispersion of magnetite in the polymer matrix. They likewise demonstrate that the covering of the oxide particles is not uniform because of non-uniform development of polymer chains. The sizes of magnetite nanoparticle were found to be in consistent with the XRD analysis results.

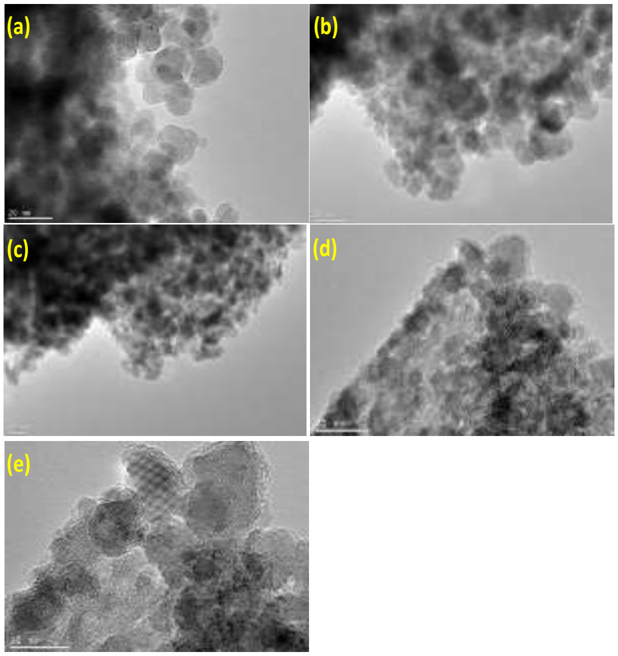

Fig. 3. TEM of (a) non-coated magnetite particles, (b) MPS-MNP1, (c) MPS-MNP2 (d) MPS-MNP5 and (e) MPS-MNP8.

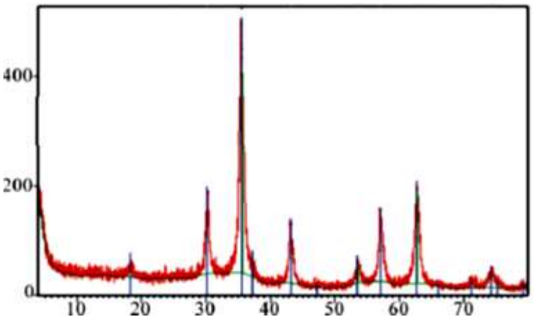

Fig. 4. XRD pattern for MPS-MNP1.

XRD analysis

Fig. 4 shows XRD pattern for MPS-MNP1 as a selected sample due to its highest content of magnetite. It can be seen that there is one sharp peak and several weak diffraction peaks. This reveals that the resultant nanoparticle contains Ferric oxide in its core and confirming its high magnetite content.

Table 5. Effect of monomer and initiator concentrations on grafting polymerization.

AAC concentration	Grafting yield	Grafting efficiency	Initiator concentration	Grafting yield	Grafting efficiency
0.5	10	65	0.01	5	60
1	20	75	0.03	30	80
1.5	40	85	0.05	10	70

Factors affecting graft polymerization

The effect of monomer and initiator concentrations on grafting polymerization is shown in **Table 5**. The data reveals that grafting yield and grafting efficiency increase by increasing AAc contents. This may be attributed to that, as monomer concentration increases the active site of grafted starch increases. On the other hand, grafting yield and grafting efficiency increase by increasing initiator concentration from 0.01 to 0.03 % and decreases by increasing imitator content to 0.05 %. This was because of increase in the active sites on starch at optimum value of initiator. Moreover, the increase in initiator concentration leads to homopolymerization due to increase in number of active radical species, which results in decrease in grafting [**34**].

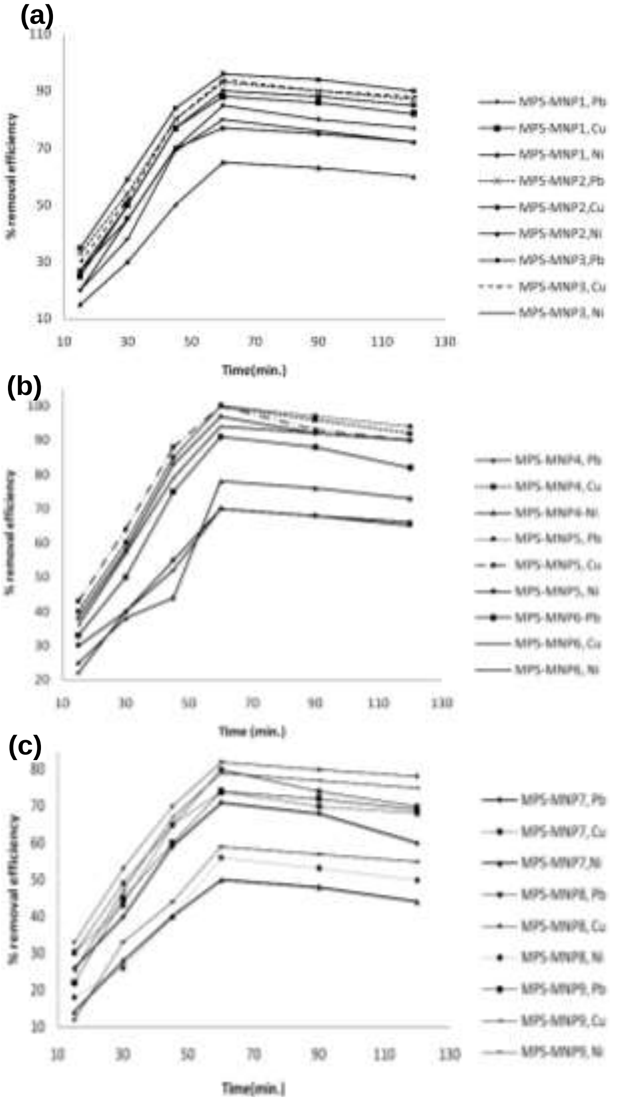

Fig. 5. (a) Contact time effect on removal efficiency of MPS-MNP (1-3) at pH 5.5 and at 35°C, (b) contact time effect on removal efficiency of MPS-MNP (4-6) at pH 5.5 and at 35°C and (c) contact time effect on removal efficiency of MPS-MNP (7-9) at pH 5.5 and at 35°C.

Factors affecting removal efficiency

Effect of contact time

Fig. 5(a-c) show absorption isotherms of Pb^{2+}, Ni^{2+} and Cu^{2+}ions adsorbed by a constant concentration of the substrate (50 mg/L) for MPS-MNPs. It is obvious that there is rapid binding of the metal to the sorbent followed by slow increase until a state of equilibrium in 60 minutes was reached. Equilibrium time is one of the vital parameters for an inexpensive wastewater treatment method. After equilibrium state, a slight decrease in the adsorption efficiency was observed and it may be due to the mobilization of some adsorbed metal ions as a result of continuous shaking of the solution. It was found that MPS-MNP5 achieved complete metal removal for both $Ni^{2+}$and $Cu^{2+}$and 70 % removal for Pb^{2+}. This may be explained on the bases of ionic radii. Ni ions with the least ionic size were observed to have adsorbed at a faster rate followed by Copper ions then Lead ions. Consequently, the smaller the ionic size, the better its affinity to reactive sites. It is possible that the metal with smaller ionic size would diffuse quicker through the adsorbent pores than the bigger ions like Pb^{2+}. Thus the adsorption of cations with larger ionic radii would be less likely compared with smaller ionic radii. Our findings run parallel to those obtained by Han and Lim [**35**]. They stated that during sorption of metal ions, the ions of smaller ionic radii tend to move faster to potential adsorption. This has been observed on other biological adsorbents as reported earlier [**35, 36**]. On the base of the structure of sorbents, it was found that there is an optimum concentration of monomer and crosslinker to attain maximum efficiency of metal removal above and below which the metal ion uptakes decreases.

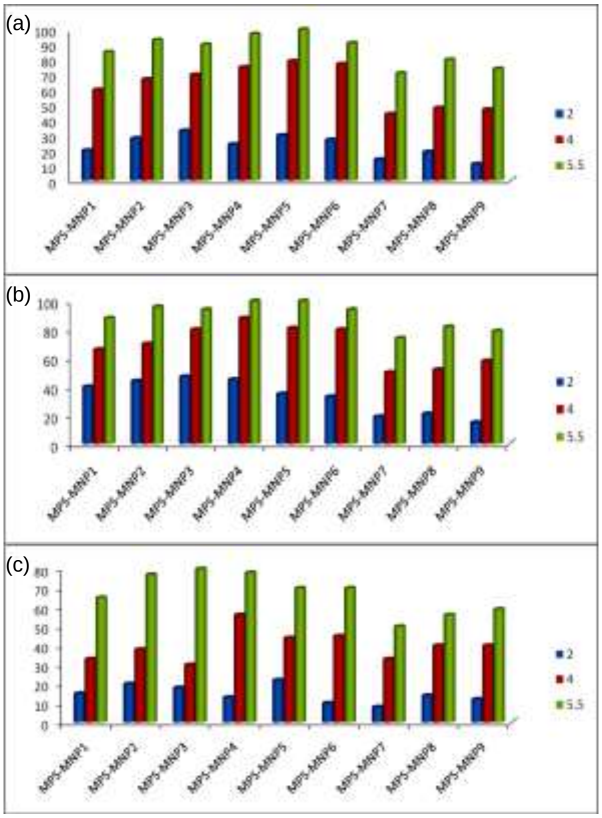

Fig. 6. (a) pH effect on removal efficiency (%) of MPS-MNPs for removal of Cu ions at 35°C, (b) pH effect on removal efficiency (%) of MPS-MNPs for removal of Ni ions at 35°C and (c) pH effect on removal efficiency (%) of MPS-MNPs for removal of Pb ions at 35°C.

Effect of pH

The pH of the aqueous solution is an important operational parameter in the adsorption process because it affects the solubility of the metal ions, concentration of the counter ions on the functional groups of the sorbent and the degree of ionization of the sorbent during the reaction. The active sites on the sorbent can either be protonated or deprotonated depending on the pH while at the same time the sorbent speciation in a solution also depends on the pH.

The effect of solution pH on the adsorption of metal ions by MPS-MNPs was studied at pH values 2, 4 and 5.5, 35 °C, and an initial ion concentration of 50 mg/L, **Fig. 7**(**a-c**). The adsorption studies at pH > 6 were not conducted due to the precipitation of Cu $(OH)_2$ from the solution. As shown in **Fig. 6**(**a-c**), there is an obvious sharp decrease in the adsorption effectiveness for all the prepared nanosorbents when the acidity of the solution increases, i.e. from pH 5.5 to pH 4 to pH 2. This low adsorption efficiency at lower pH value could be referred to the sufficiently high hydrogen ion concentration, which led to the strong competitive adsorption [**36**]. Our findings match those obtained by Francesca *et al.* [**37**]. It can also observed that the order of metal ion uptake is Ni^{2+}> Cu $^{2+}$> Pb^{2+}. The set of nanosorbents that have complete polymer coating around the magnetic nanoparticles showed the best performance. This finding agrees with the data obtained from TEM images.

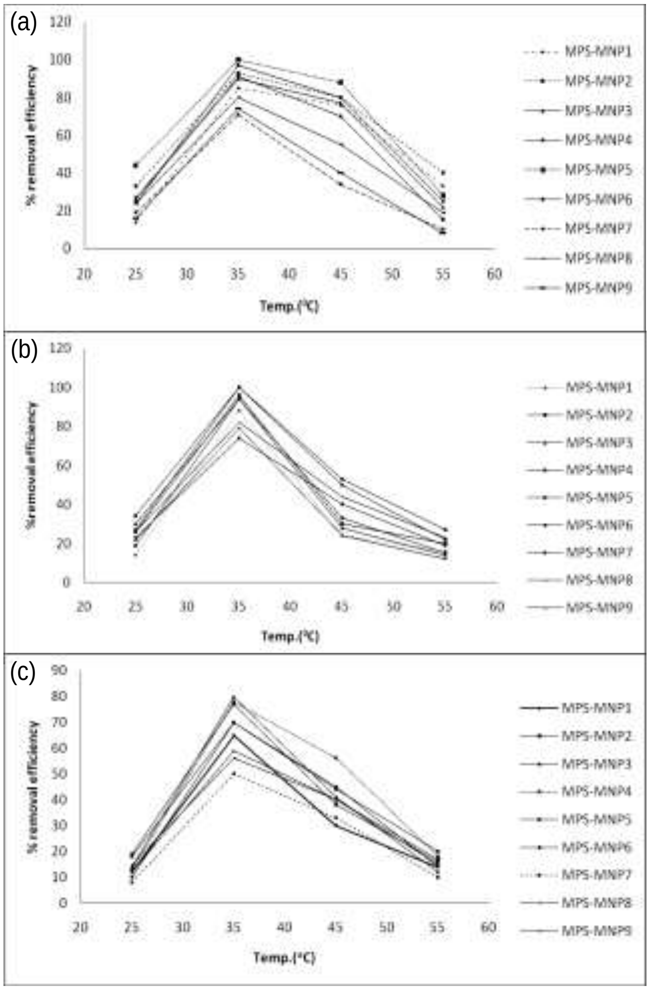

Fig. 7. (a) Temperature effect of on removal efficiency (%) of MPS-MNPs for removal of Cu ions at pH 5.5, (b) Temperature effect of on removal efficiency (%) of MPS-MNPs for removal of Ni ions at pH 5.5 and (c)Temperature effect of on removal efficiency (%) of MPS-MNPs for removal of Pb ions at pH 5.5.

Effect of temperature

Temperature effects on the elimination of metal ions by MPS-MNPs were studied at aqueous solution of pH 5.5 and at temperature range 25-55 °C and an initial metal ion concentration of 50 mg/L. As shown in **Fig. 7**(**a-c**), it was found that the removal efficiency in percentage for the biosorbents increased by increase the temperature from 25 to 35 °C, revealing that, the adsorption process was endothermic. But there is a sharp decrease in the efficiency above 35 °C. One possible explanation was that the metal ions were well hydrated. They have to lose part of hydration sheath in order to be adsorbed. This dehydration process of metal ions needed energy [**38**]. At higher temperatures, some desorption occurs due to the shrinkage of the sorbent and release some of the absorbed ions resulting in increasing the ion concentration in the solution again.

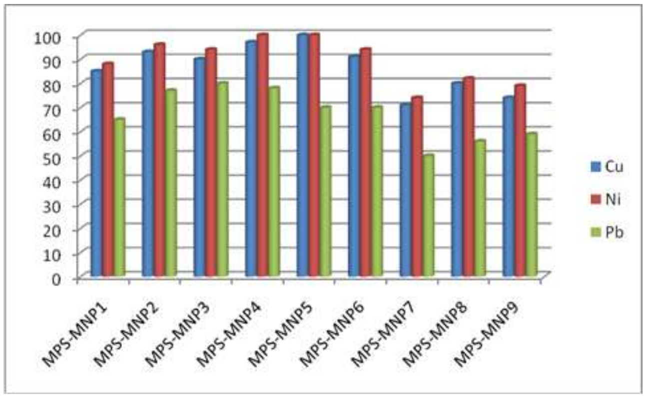

Fig. 8. Competitive adsorption experiment for the prepared MPS-MNPs sorbents.

Competitive adsorption

The selectivity of MPS-MNPs sorbents towards specific metal ion was investigated by preparing of stock solution containing equal concentrations of the three investigated metal ions at optimum adsorption conditions. As shown in **Fig. 8**, the adsorption efficiency of the biosorbents towards Ni and Cu ions is more pronounced. The uptake of Pb ions is much lower than the other two metal ions. This finding may be attributed to the smaller ionic size of both Ni and Cu ions relative to Pb ions. Jimoh *et al.* [**39**] stated that the order of removal of heavy metals by some cellulosic biosorbents was Mn (II)>Pb (II) due to difference in ionic sizes.

Reusability of the prepared biosorbents

Sorption-desorption experiments were carried out four rounds in order to investigate the reusability of the prepared sorbents. The data obtained from these experiments are illustrated in **Fig. 9**(**a-c**) for Ni, Cu and Pb ions respectively. It is obvious that the elimination efficiency of the modified potato starch sorbents was the same in the first and second rounds followed by slight decrease in the third round then remarkable decrease in the last round. This may be explained by the decomposition of parts of gel structure by the desorbing effluent [**40, 41**]. This finding proves the economic importance of the modified potato starch for two reasons. First, they were prepared from abundant natural waste material and second they are reusable several times with reasonable efficiency.

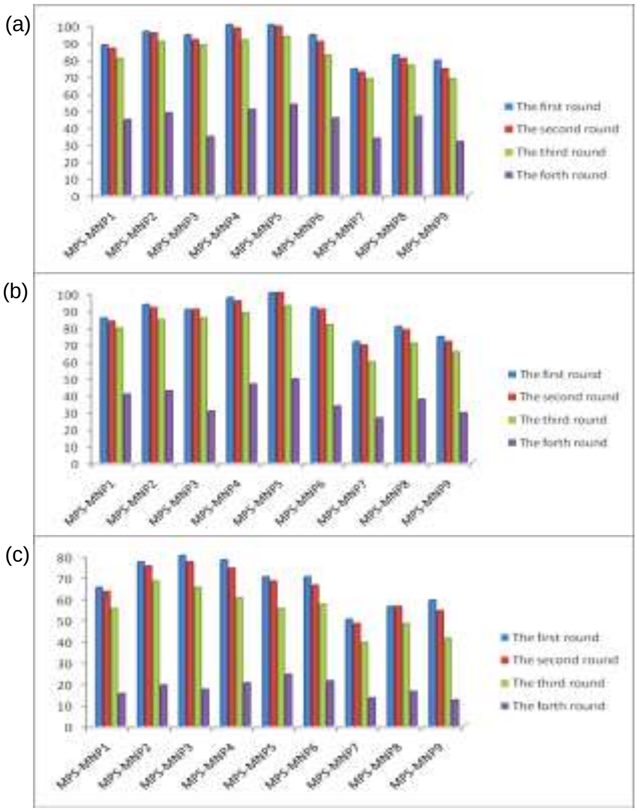

Fig. 8. (a) Reusability MPS-MNPs in removal of Ni ions at four rounds, (b) reusability MPS-MNPs in removal of Cu ions at four rounds and (c) reusability MPS-MNPs in removal of Pb ions at four rounds.

Conclusion

Treated potato starch was grafted with different weight ratios of acrylic acid in presence of different ratios of benzoyl peroxide as crosslinker. The grafted potato starch was then fabricated with iron oxide to prepare modified potato starch magnetic nano particles, MPS-MNPs. The nanosorbents were used as biosorbents in order to eliminate some heavy metals from waste water. The obtained data revealed that the biosorbents were effective in removing Nickel, Copper and Lead from waste water. It was found that the removal efficiency was dependent on several factors such as temperature at which the sorbents applied pH of the medium and the contact time between the metal ions and the sorbents. The data showed that the maximum removal efficiency was achieved at pH 5.5 and temperature 35 ^{o}C.

Reference

1. Oghenerobor B. A.; Gladys O. O.; Tomilola D. O.; *Advances in Bioscience and Bioengineering*, **2014**, *2*, 37.
DOI: 10.11648/j.abb.20140204.11
2. Gupta, N.; Kushwaha, A. K.; Chattopadhyaya, M. C., *Journal of the Taiwan Institute of Chemical Engineers* **2012**, *43*, 125.
DOI: 10.1016/j.jtice.2011.07.009
3. Heidari, A.; Younesi, H.; &Mehraban, Z. *Chemical Engineering Journal* **2009**,*153*, 70.
DOI: 10.5829/idosi.ije.2013.26.05b.03
4. Fernández, M.; Villalonga, M. L.; Fragoso, A.; Caob, Banos, M., Villalonga, R. *Process Biochemistry* **2004**, *39*, 535.
DOI: 10.1016/S0032-9592(03)00069-4
5. Futalan, C. M.; Kan, C. C.; Dalid, M. L.; Hsien, K. J.; Pascua, C.; Wan, M. W.; *Carbohydrate Polymers* **2011**, *83*, 528.
DOI: 10.6088/ijes.2013040100012
6. Gupta, V. K.; Nayak, A. *Chemical Engineering Journal* **2012**, *180*, 81.
DOI: 10.1016/j.cej.2011.11.006
7. Gupta, V. K.; Rastogi, A., *Journal of Hazardous Materials*, **2009**, 163, 396.
DOI: 10.1016/j.jhazmat.2008.06.104.
8. Abdullah K.; Nabil, H.; Sakr, M.; *Environmental Science pollution research* **2012**, *19*, 2832.
DOI: 10.1007/s11356-012-0788-1
9. Ayoub, A. S.; Rizvi, S. S. H.; *Journal of Plastic Film and Sheeting* **2009**, *25*, 25.
DOI: 10.1177/8756087909336493
10. Crini, G. *Progress in Polymer Science* **2005**, *30*, 38.
DOI: 10.1016/j.progpolymsci.2004.11.002
11. Mahmood N.; Ladan R.; Fereshteh Z.; *Chemical Speciation and Bioavailability* **2014**, *26*.
DOI: 10.3184/095422914X14039722451529
12. Feng, Y.; Gong, J. L.; Zeng, G. M.; Niu, Q. Y.; Zhang, H. Y.; Niu, C. G. *Chemical Engineering Journal* **2010**, *162*, 487.
DOI: 10.1016/j.cej.2010.05.049
13. Tran, H. V.; Tran, L. D.; & Nguyen, T. N. *Materials Science and Engineering* **2010**, *30*, 304.
DOI: 1016/j.msec.2009.11.008
14. Banerjee, S. S.; Chen, D. H. *Journal of Hazardous Materials* **2007**,*147*, 792.
DOI: 10.1016/j.jhazmat.2007.01.079
15. Alexis W. C.; Charles F.de L.; Mark R. W. *Environ. Sci Technol*. **2015**, *49*, 5277.
DOI: 10.1021/es506351r
16. Nejat S. Behbahani, K. R.; Mohammad R. Y., Abbasali Z.; Hamideh A. *Environ Health Sci Eng*.**2014**, *12*, 103.
DOI: 10.1186/2052-336X-12-103
17. Barakat M. A. *Journal of Environmental Science and Technology*, **2008**, *1*,151.
DOI: 10.3923/jest.2008.151.156
18. Kim, M.; Lee, S.J.; *Carbohydrate Polymers* **2002**, *50*, 331.
DOI: 10.5402/2012/348685
19. Pourjavadi, A.; Ayyari, M.; Amini-Fazl, M. S. *European Polymer Journal* **2008**, *44*, 1209.
DOI: 10.1016/j.eurpolymj.2008.01.032
20. Reez A.; Rajeef K.; Haseeb Kh.; *Arabian Journal of Chemistry* **2012**, *5*, 353.
DOI: 10.1016/j.arabjc.2010.09.003
21. Crini, G. *Progress in Polymer Science* **2005**, *30*, 38.
DOI:10.1016/j.progpolymsci.2004.11.002
22. Song, H.; Wu, D.; Zhang, R.Q.; Qiao, L.Y.; Zhang, S. H.; Lin, S.; Ye, *J. Carbohydr. Polym*. **2009**, *78*, 253.
DOI: 10.1016/j.carbpol.2009.03.027
23. Khairkar, Shyam R.; Raut, Arun R.; *Science Journal of Analytical Chemistry* **2014**, *2*, 67.
DOI: 10.11648/j.sjac.20140206.12
24. N. Dave, P.; Chopda, Lakhan V. *Journal of Nanotechnology* **2014**, Article ID 398569, 14.
DOI:10.1155/2014/398569
25. Liu, Y.; Wang, W.; & Wang, A. Desalination, **2010**, *259*, 258.
DOI: 10.1016/j.desal.2010.03.039
26. Muggundha, R.; Sharifah, M.; Mhd, R. *Int J. Mol Sci*.**2014**, *15*,100.
DOI: 10.3390/ijms15010100
27. Deepak P.; Reena Sh. and Susheel K.; *Adv. Mat. Lett.* **2012**, *3*, 259.
DOI: 10.5185/amlett.2012.3328
28. Lu, D. R.; Xiao, C. M.; Xu, S. J. *Express Polymer Lett.* **2009**, *3*, 366.
DOI: 10.3144/expresspolymlett.2009.46
29. Kumari, A.; Kaith, B. S.; Singh, A. S.; Kalia, S. *Advanced Materials Letters* **2010**, *1*, 23.
DOI: 10.5185/amlett.2010.6129
30. Egila, J. N.; Dauda, B. E. N.; Iyaka, Y. A.; Jimoh, T. *International Journal of the Physical Sciences* **2011**, *6*, 2152.
DOI: 10.5897/IJPS10.251

31. Mingzku, L.; Rongshi, C.; Jingjia, W.; Cheng, M. J. *Polym. Sci. Polym. Chem.* **1993**, *31*, 3181.
    DOI: 10.1002/app.20883
32. Lai, S. M.; Don, T. M.; Liu, Y. H.; Chiu, W. Y. J. *Appl. Polym. Sci.* **2006**, *102*, 3017.
    DOI: 10.1002/app.24672
33. Badruddoza, A. Z. M.; Tay, A. S. H.; Tan, P. Y.; Hidajat, K.; Uddin, M. S. *Journal of Hazardous Materials* **2011**, *185*, 1177.
    DOI:10.1016/j.jhazmat.2010.10.029
34. Pathania, D.; Sharma, R. Synthesis and characterization of graft copolymers of methacrylic acid onto gelatinized potato starch using chromic acid initiator in presence of air, *Adv. Mat. Lett.***2012**, *3*, 136.
    DOI: 10.5185/amlett.2011.8297
35. Han, J. A.; Lim, S. T. *Carbohydrate Polymers* **2004**, *55*, 193.
    DOI: 10.1016/j.carbpol.2003.09.006
36. Qiu Y.; Cheng H.; Xu C.; Sheng S. D. *Water Res.* **2008**, *42*, 567.
    DOI: 10.1016/j.watres.2007.07.051
37. Francesca P.; Sara M.; Luigi T.; *Water Res.* **2008**, *42*, 2953.
    DOI: 10.1016/j.watres.2008.03.012.
38. Abdel-Raouf M.; Abdul-Raheim A.; El-Kafrawy A.; Maysour N.; Ibraheim A.; Abdel-Azim A.; *International Journal of Chemistry and Material Science* **2013,** *1*, 36.
    ISSN: 2327-5553
39. Jimoh, T. O.; Buoro, A. T.; Murian, M.; *Journal of Environmental Chemistry and Ecotoxicology* **2012**, 4, 178.
    DOI: 10.5897/JECE12.015
40. Pushpendra K. Sh.; Sohail A.; Chandra N. T.; *International Refereed Journal of Engineering and Science (IRJES)* **2013**, *2*,18.
    ISSN: 2319-183X
41. Amuda, O. S.; Amoo, I. A. *J. Haz. Mater.* **2006**, *747*, 778.
    DOI: 10.1016/j.jhazmat.2006.07.044

.